Systematized calculation of optimal coefficients of 3-D chamfer norms

Céline Fouard, Grégoire Malandain

▶ **To cite this version:**

Céline Fouard, Grégoire Malandain. Systematized calculation of optimal coefficients of 3-D chamfer norms. Discrete Geometry for Computer Imagery, 2003, Napoli, Italy. pp.214–223, 10.1007/b94107 . hal-00308962

HAL Id: hal-00308962
https://hal.science/hal-00308962

Submitted on 5 Aug 2008

HAL is a multi-disciplinary open access archive for the deposit and dissemination of scientific research documents, whether they are published or not. The documents may come from teaching and research institutions in France or abroad, or from public or private research centers.

L'archive ouverte pluridisciplinaire **HAL**, est destinée au dépôt et à la diffusion de documents scientifiques de niveau recherche, publiés ou non, émanant des établissements d'enseignement et de recherche français ou étrangers, des laboratoires publics ou privés.

Systematized calculation of optimal coefficients of 3-D chamfer norms

Céline Fouard[1,2,3] and Grégoire Malandain[1]

[1] Epidaure Research Project, INRIA Sophia Antipolis, France
[2] TGS Europe SA, PA Kennedy 1 - BP 227 F-33708 Merignac Cedex
[3] INSERM U455 Toulouse

Abstract. Chamfer distances are widely used in image analysis, and many ways have been investigated to compute optimal chamfer mask coefficients. Unfortunately, these methods are not systematized: they have to be conducted manually for every mask size or image anisotropy. Since image acquisition (e.g. medical imaging) can lead to anisotropic discrete grids with unpredictable anisotropy value, automated calculation of chamfer mask coefficients becomes mandatory for efficient distance map computation. This article presents a systematized calculation of these coefficients based on the automatic construction of chamfer masks of any size associated with a triangulation that allows to derive analytically the relative error with respect to the Euclidean distance, in any 3-D anisotropic lattice.
Keywords: chamfer distance, anisotropic lattice

1 Introduction

Distance transformations (DTs) are widely used in image analysis since they allow to recover morphometric features of a binary shape. Among other applications, they can be applied to skeleton computation [1], Voronoï diagram construction, or shape-based interpolation [2]. Distance transformation transforms a binary image into a grey level image where the value of each foreground pixel corresponds to its shortest distance to the background. Brute-force computation of DT is not compatible with expected image analysis requirements, so DTs are usually computed by propagation. Exact Euclidean maps can be computed through Euclidean Distance Transformations (EDT). Several EDT have been proposed, using morphological operators [3, 4], filters [5], several path on rows and columns [6], or propagating vectors [7, 8], but lead to time and/or memory consuming algorithms. A good trade-off between precision and computational cost for DT is achieved by chamfer maps that have been made popular by Borgefors [9]. These maps are computed through two raster-scan on the image that propagate the distance values by the way of chamfer masks. The coefficients of the mask are (proportional) estimation of short-range distances: the larger the chamfer mask is, the closest to the Euclidean map the chamfer map will be. The calculation of optimal coefficients can be done by minimizing either an absolute error [10] or a relative one [11]. It has first been done for 2-D 3×3 masks

[10] in isotropic lattices, then extended to larger masks [9, 11] and to higher dimensions [12]. Anisotropic lattices have also been considered [13–15]. However, those calculations remain tedious and are not systematized: thus they have to be conducted manually for every mask size or anisotropy value.

Our motivation is the computation of DT in 3-D medical images: they are usually acquired on anisotropic lattices (slice thickness is usually larger than the pixel size) and this anisotropy may vary from one acquisition to the other. The efficient computation of chamfer maps requires then the calculation of the chamfer mask's coefficient to be automated. calculation of these coefficients for any mask size and any anisotropy value. In addition to classical error criteria, we also consider norm constraints [16] that guarantee predictable results. Our approach is based on the automatic construction of chamfer masks of any size associated with a triangulation that allows to derive analytically the relative error with respect to the Euclidean distance.

In the following, we first recall some basic definitions. Then we describe error estimation and norm constraints. Some results (coefficients of isotropic 7^3 and anisotropic 3^3 masks) are given before we conclude.

2 Definitions and notations

We recall here some notations and definitions. We consider the discrete space $\mathbb{E} = \mathbb{Z}^3$. An image I is an application defined on $\mathbb{E}$.

A *discrete distance* is an application $d : \mathbb{E} \times \mathbb{E} \longrightarrow \mathbb{N}$ that verifies for all $p, q, r \in \mathbb{E}$ the following 4 properties:

$$\begin{array}{lll} d(p) \geq 0, & & d(p,q) = 0 \Longleftrightarrow p = q, \\ d(p,q) = d(q,p), & \text{and} & d(p,q) \leq d(p,r) + d(r,q). \end{array}$$

Given a discrete distance d, the application $n : \mathbb{E} \longrightarrow \mathbb{N}$ is a *discrete norm* on $\mathbb{Z}$ if and only if $\forall p \in \mathbb{E}, n(\lambda p) = |\lambda| n(p)\ \forall \lambda \in \mathbb{Z}$.

Let us consider a binary image I with foreground X and background $\overline{X}$. The *distance map* D_X is an application defined on $\mathbb{E}$ such that $D_X(p) = \inf_{q \in \overline{X}} d(p,q)$.

Distance maps can be approximated by chamfer maps, that can be computed with a two-passes (so-called forward and backward passes) algorithm [17]. To do so, we need to define the *chamfer mask* which is a set $\mathcal{M}_C = \{(\mathbf{v_i}, \omega_i),\ 1 \leq i \leq m\}$ of weighted vectors representing authorized displacements. It is centered in O, symmetrical with respect to its center and contains at least a base of $\mathbb{E}$.

Given a chamfer mask $\mathcal{M}_C$ and two points $p, q \in E$, we define a *path* $\mathcal{P}_{pq}$ from A to B as a sequence of vectors $\mathbf{v_i} \in \mathcal{M}_C$ so that $\overrightarrow{pq}$ is expressed as a linear combination of vectors: $\overrightarrow{pq} = \sum n_i.\mathbf{v_i}$ with $n_i \in \mathbb{N}$. The *cost* W of a path $\mathcal{P}_{pq}$ is defined as $W(\mathcal{P}_{pq}) = \sum n_i.\omega_i$. The chamfer distance between two points $p, q \in E$ as the minimal possible cost, *i.e.* $d_C(p,q) = \min_{\mathcal{P}_{pq}} W(\mathcal{P}_{pq})$.

3 Computing optimal coefficients for chamfer norms

Calculating the optimal weights for a given chamfer mask is usually achieved by minimizing the error (either absolute or relative) between the chamfer's distance

and the Euclidean one. Thanks to symmetry considerations, we can only consider the *mask generator* $\mathcal{M}_C^g$, *i.e.* the part of the anisotropic chamfer mask $\mathcal{M}_C$ that is included in the first eighth of the space, $\frac{1}{8}\mathbb{Z}^3$, delimited by the half-lines $(O, \mathbf{x})$, $(O, \mathbf{y})$ and $(O, \mathbf{z})$. Moreover, vectors are also chosen so that $\forall i, j$ with $i \neq j$, $\nexists n \in \mathbb{N}$ such that $\mathrm{v}_i = n\mathrm{v}_j$.

Estimating the error between a chamfer distance and the Euclidean one is quite awkward when dealing with large masks. This difficulty can be reduced if we are able to *triangulate* the mask generator $\mathcal{M}_C^g$ into *regular cones*.

A *continuous cone*, defined by a triplet of vectors and denoted by $\langle \mathbf{v_i}, \mathbf{v_j}, \mathbf{v_k} \rangle$, represents the region of $\mathbb{R}^3$ delimited by the vectors $\mathbf{v_i}$, $\mathbf{v_j}$ and $\mathbf{v_k}$, *i.e.*

$$\langle \mathbf{v_i}, \mathbf{v_j}, \mathbf{v_k} \rangle \triangleq \{M \in \mathbb{R}^3 | \overrightarrow{OM} = \lambda_i.\mathbf{v_i} + \lambda_j.\mathbf{v_j} + \lambda_k.\mathbf{v_k},\ \lambda_i, \lambda_j, \lambda_k \in \mathbb{R}^+\}$$

A *discrete cone*, $\langle\langle \mathbf{v_i}, \mathbf{v_j}, \mathbf{v_k} \rangle\rangle$, is the set of points of $\mathbb{Z}^3$ that are included in the continuous cone $\langle \mathbf{v_i}, \mathbf{v_j}, \mathbf{v_k} \rangle$: $\langle\langle \mathbf{v_i}, \mathbf{v_j}, \mathbf{v_k} \rangle\rangle \triangleq \{M \in \mathbb{Z}^3 | M \in \langle \mathbf{v_i}, \mathbf{v_j}, \mathbf{v_k} \rangle\}$. A *regular cone* is a discrete cone that verifies $\Delta_{i,j,k} = \pm 1$ where $\Delta_{i,j,k}$ is the determinant of the matrix $|\mathbf{v_i}\mathbf{v_j}\mathbf{v_k}|$ (first column is vector $\mathbf{v_i}$, etc). Regular cones have the interesting properties that any point of the cone can be expressed in the basis of the 3 vectors defining the cone, *i.e.*

$$\langle\langle \mathbf{v_i}, \mathbf{v_j}, \mathbf{v_k} \rangle\rangle = \{M \in \mathbb{Z}^3 | \overrightarrow{OM} = \lambda_i.\mathbf{v_i} + \lambda_j.\mathbf{v_j} + \lambda_k.\mathbf{v_k},\ \lambda_i, \lambda_j, \lambda_k \in \mathbb{N}\}$$

only holds for regular cones [18]. Having a mask generator that can be triangulated into regular cones allows us to reduce the calculation of the error into independent calculations in each regular cone. In the following, we will only deal with such mask generators. To ensure that they can be triangulated into regular cones, we build them with the Farey triangulation [16]. This technique allows us to recursively (and automatically) built large mask generators $\mathcal{M}_C^g$ with their associated regular triangulation $\mathcal{T}_C^g = \{\langle\langle \mathbf{v_i}, \mathbf{v_j}, \mathbf{v_k} \rangle\rangle\}$ (see appendix A).

3.1 Error definition and calculation

We have chosen to minimize the relative error between the chamfer distance and the Euclidean one, computed on planes $x = \text{cste}$, or $y = \text{cste}$, or $z = \text{cste}$.

Let us consider a point $P = (x, y, z)$. According to above section, we know that its chamfer distance to the origin O, denoted $d_C(P)$, is a linear combination of the weights of the 3 vectors defining the regular cone it belongs to. We have then $d_C(P) = a.\omega_i + b.\omega_j + c.\omega_k$ with $\overrightarrow{OP} = a.\mathbf{v_i} + b.\mathbf{v_j} + c.\mathbf{v_k}$. Solving the latter expression yields (recall that $\Delta_{i,j,k} = \pm 1$ for regular cones)

$$a = \frac{1}{\Delta_{i,j,k}} \begin{vmatrix} x & x_j & x_k \\ y & y_j & y_k \\ z & z_j & z_k \end{vmatrix}, \quad b = \frac{1}{\Delta_{i,j,k}} \begin{vmatrix} x_i & x & x_k \\ y_i & y & y_k \\ z_i & z & z_k \end{vmatrix}, \quad \text{and } c = \frac{1}{\Delta_{i,j,k}} \begin{vmatrix} x_i & x_j & x \\ y_i & y_j & y \\ z_i & z_j & z \end{vmatrix}$$

and allows us to obtain $d_C(x, y, z) = \alpha.x + \beta.y + \gamma.z$ with

$$\begin{aligned} \alpha &= (y_j z_k - y_k z_j).\omega_i + (y_k z_i - y_i z_k).\omega_j + (y_i z_j - y_j z_i).\omega_k \\ \beta &= (z_j x_k - z_k x_j).\omega_i + (z_k x_i - z_i x_k).\omega_j + (z_i x_j - z_j x_i).\omega_k \\ \gamma &= (x_j y_k - x_k y_j).\omega_i + (x_k y_i - x_i y_k).\omega_j + (x_i y_j - x_j y_i).\omega_k \end{aligned}$$

Chamfer distances are usually computed with integer weights, and have to be scaled with a real factor, ε (typically the displacement associated with the smallest voxel size), to be compared to the Euclidean distance $d_E(x,y,z) = \sqrt{d_x^2x^2 + d_y^2y^2 + d_z^2z^2}$ where d_x, d_y and d_z denote the voxel size in the $\mathbf{x}$, $\mathbf{y}$, and $\mathbf{z}$ direction. The relative error to minimize is then defined by

$$E_{relative}(x,y,z) = \frac{d_C/\varepsilon - d_E}{d_E} = \frac{1}{\varepsilon}\frac{\alpha.x + \beta.y + \gamma.z}{\sqrt{d_x^2x^2 + d_y^2y^2 + d_z^2z^2}} - 1. \quad (1)$$

Depending on the orientation of the cone, this error has to be minimized on either the plane $x = M$, or $y = M$, or $z = M$. Without loss of generality, we will only go into details for the case $x = M$,$M \neq 0$. The error has then to be estimated on the triangle defined as the intersection between the cone $\langle \mathbf{v}_i, \mathbf{v}_j, \mathbf{v}_k \rangle$ and the plan $x = M$. The vertices of this triangle are the points $V_l = (M, M\frac{y_l}{x_l}, M\frac{y_l}{x_l}) = (M, y'_l, x'_l)$ for $l = i, j, k$. In plane $x = M$, the relative error can be rewritten

$$E_x(y', z') = \frac{1}{\varepsilon}\frac{\alpha + \beta.y' + \gamma.z'}{\sqrt{d_x^2 + d_y^2y'^2 + d_z^2z'^2}} - 1 \quad \text{with } y' = \frac{y}{M} \text{ and } z' = \frac{z}{M}. \quad (2)$$

E_x is continuous on a closed and bounded interval (the triangle $V_iV_jV_k$), it is then bounded and reaches its bounds. Its extrema can be located either inside the triangle, or on the edges of the triangle, or at the vertices of the triangle. Let us consider the three cases.

1. The extremum is inside the triangle. By derivating equation 2, it comes that the extremum will be located at $(y'_{max}, z'_{max}) = \left(\frac{\beta d_x^2}{\alpha d_y^2}, \frac{\gamma d_x^2}{\alpha d_z^2}\right)$. If this point is inside the triangle $V_iV_jV_k$, it yields an extreme value

$$E_x(V_iV_jV_k) = \frac{1}{\varepsilon}\sqrt{\frac{\alpha^2}{d_x^2} + \frac{\beta^2}{d_y^2} + \frac{\gamma^2}{d_z^2}} - 1.$$

2. The extremum is on an edge. There are three edges, but we will only present the calculation for V_iV_j. In this case, a point M belonging to the edge can be represented by $M = aV_i + (1-a)V_j$ yielding the relative error along the edge

$$E_x(a) = \frac{1}{\varepsilon}\frac{(\beta.Y+\gamma.Z)a+(\alpha+\beta.y_j+\gamma.z_j)}{\sqrt{(d_y^2Y^2+d_z^2Z^2)a^2+2(d_y^2y_jY+d_z^2z_jZ)a+d_x^2+d_y^2y_j^2+d_z^2z_j^2}} - 1 \text{ with } \begin{cases} Y = y_i - y_j \\ Z = z_i - z_j \end{cases}. \quad (3)$$

After derivation, it can be shown that the extreme value is reached for

$$a_{max} = -\frac{(\beta(y_jZ - z_jY) + \alpha Z)z_jd_z^2 + (\gamma(z_jY - y_jZ) + \alpha Y)y_jd_y^2 - (\beta Y + \gamma Z)d_x^2}{(\beta(y_jZ - z_jY) + \alpha Z)Zd_z^2 + (\gamma(z_jY - y_jZ) + \alpha Y)Yd_y^2}.$$

If $0 \leq a_{max} \leq 1$, the extreme value $E_x(V_iV_j)$ is given by $E_x(a_{max})$ whose form is not simple enough to be displayed here.

3. The extremum is reached on one of the triangle's vertices, V_l where the relative error value is given by

$$E_x(V_l) = \frac{1}{\varepsilon}\frac{\omega_l}{||\mathbf{v_l}||_{\mathbb{R}}} - 1 \quad \text{with } ||\mathbf{v_l}||_{\mathbb{R}} = \sqrt{x_l^2 d_x^2 + y_l^2 d_y^2 + z_l^2 d_z^2}$$

Thus we are now able to compute both the minimum and maximum relative errors, τ_{min} and τ_{max} (please recall that they depend on ε), for a mask generator $\mathcal{M}_C^g$ by

$$\tau_{min} = \min_{\langle\langle \mathbf{v_i},\mathbf{v_j},\mathbf{v_k}\rangle\rangle \in \mathcal{T}_C^g} \min\left(E_u(V_iV_jV_k), \min_{l,m} E_u(V_lV_m), \min_{l} E_u(V_l)\right)$$

$$\tau_{max} = \max_{\langle\langle \mathbf{v_i},\mathbf{v_j},\mathbf{v_k}\rangle\rangle \in \mathcal{T}_C^g} \max\left(E_u(V_iV_jV_k), \max_{l,m} E_u(V_lV_m), \max_{l} E_u(V_l)\right)$$

u denoting the plane (x, y, or z) where the error is minimized; $E_u(V_iV_jV_k)$ and $E_u(V_lV_m)$ being estimated only if the corresponding extremum lies in the correct interval.

The global relative error is defined by $\tau(\varepsilon) = \max(\tau_{min}(\varepsilon), \tau_{max}(\varepsilon))$. According that $\tau_{min}(\varepsilon) < 0$ and $\tau_{max}(\varepsilon) > 0$, we can make them equal in absolute value by changing the value of ε into $\varepsilon_{opt} = \varepsilon\left(\frac{\tau_{min}+\tau_{max}}{2} + 1\right)$ [19]. We obtain the optimal relative error τ_{opt} by $\tau_{opt} = -\tau_{min}(\varepsilon_{opt}) = \tau_{max}(\varepsilon_{opt})$.

3.2 Norm constraints

It can be shown that the chamfer distance d_C induced by any chamfer mask $\mathcal{M}_C$ is a discrete distance [20]. However, a distance that is not a norm is not invariant by homothety and this may not be desirable (for instance when comparing skeletons of the same object at different scales). Therefore, we introduce additional criteria to ensure that the computed weights will define a discrete norm.

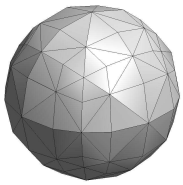

Fig. 1. Equivalent rational ball of a 3D $5 \times 5 \times 5$ isotropic chamfer mask.

A distance is a norm if and only if its ball is convex, symmetric, and homogeneous. For chamfer masks, symmetry is achieved by construction, homogeneity is due to the regular triangulation (also obtained by construction) while convexity can be assessed on the *equivalent rational ball* of the chamfer mask [16].

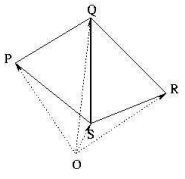

Fig. 2. Notations for equation 4.

Given a chamfer mask $\mathcal{M}_C = \{(\mathbf{v_i} \in \mathbb{Z}^3, \omega_i \in \mathbb{N})\}$ its *equivalent rational mask* is defined by $\mathcal{M}'_C = \{(\mathbf{v_i}/\omega_i \in \mathbb{Q}^3, 1)\}$. The polyhedron defined by this equivalent rational mask is the equivalent rational ball (see figure 1).

To check the convexity of the ball, we have to check whether the ball is convex at each of its edges [16]: each

edge must be "turned to the outside" of the ball. It turns out that we only have to check a *local convexity criterion* (LCC) at each edge of the equivalent rational ball. Given 2 faces (P, Q, S) and (Q, R, S) of a triangulation sharing edge (Q, S), the LCC can be expressed as

$$LCC(P,Q,R,S) = \frac{1}{\omega_P.\omega_Q.\omega_R.\omega_S}.\begin{vmatrix} x_Q & x_R & x_S & x_P \\ y_Q & y_R & y_S & y_P \\ z_Q & z_R & z_S & z_P \\ \omega_Q & \omega_R & \omega_S & \omega_P \end{vmatrix} \geq 0. \quad (4)$$

4 Automatic calculation of chamfer mask coefficients

The computation of optimal coefficients for a mask of size $(2n+1)^3$ is done in three steps: generation of the Farey triangulation, generation of the norm constraints, and iterative computation of the optimal sets of weights.

4.1 Building the Farey triangulation

The recursive automated construction of the Farey triangulation of order n is described in appendix A. This triangulation $\mathcal{T}_C^g$ corresponds to isotropic chamfer mask generator $\mathcal{M}_C^g$. When dealing with anisotropic lattice, one has to add extra vectors to the mask generator and extra cones to the triangulation.

This is achieved by symmetry considerations. For instance, for a 3^3 mask, if the voxel size d_z along z is different from the ones along x and y, d_x and d_y, we have to consider in the mask generator, in addition to the vectors $\{_{(1,0,0)}, _{(1,1,0)}, _{(1,1,1)}\}$, the two extra vectors $\{_{(0,0,1)}, _{(1,0,1)}\}$ that corresponds to weights induced by the anisotropy. These extra vectors belongs to the two extra cones, $\langle\langle_{(1,0,0)}, _{(1,0,1)}, _{(1,1,1)}\rangle\rangle$ and $\langle\langle_{(0,0,1)}, _{(1,0,1)}, _{(1,1,1)}\rangle\rangle$, that are to be considered for the error computation and the local convexity constraints.

4.2 Generating convexity criteria

The triangulation $\mathcal{T}_C^g$ has been built as described above. It allows us to generate all the local convexity constraints (equation 4) that are to be verified. They have to be generated for every edge inside the mask generator, but also for the edges that are at the border of the mask generator. For the latter, the fourth point (see figure 2) is derived from symmetry considerations.

Please notice that each of the generated LCC depends on 4 weights ω_i.

4.3 Finding the optimal coefficients

This is the tough part. We have to identify the m-tuples $(\omega_1 \dots \omega_m)$ of weights corresponding to the chamfer mask generator $\mathcal{M}_C^g = \{\mathbf{v}_i, 1 \leq i \leq m\}$ to find the optimal ones that yield optimal error.

These sets of optimal coefficients are searched by a brute-force method. However, we try to reduce this computationally expensive search by throwing away

m-tuples $(\omega_1 \dots \omega_m)$ as soon as part of them do not satisfy the local convexity constraints (as sketched by below recursive algorithm[1]).

```
 1: procedure TEST( n )
 2: if some LCCs can be verified with (ω_i, ... ω_n) then
 3:    test these LCCs and return if one of them is not verified
 4: if n equals to m then {All ω_i are set.}
 5:    Compute the error τ_opt
 6:    if this τ_opt is smaller than the previous one then
 7:       (ω_i, ..., ω_m) is an optimal set of coefficients
 8:    return
 9: for ω_{n+1} from ω_1||v_i||_∞ to ω_1||v_i||_1 do {Iteratively set a value to ω_{n+1}.}
10:    TEST( n + 1 )
11: {Main Program}
12: for ω_1 from 1 to some user provided value do
13:    TEST( 1 )
```

ω_1, the coefficient corresponding to the direction of smallest voxel size, varies from 1 to some maximal value provided by the user, while the other coefficients are searched in the interval $[\omega_1||\mathbf{v_i}||_\infty, \omega_1||\mathbf{v_i}||_1]$. Error computation is only performed on coefficients sets that verify all the local convexity constraints. As a result, this algorithm gives all the optimal m-tuples in lexicographical order.

aX	aY	aZ	bYZ	bXZ	bXY	c	ε_{opt}	$\tau_{opt}(\%)$
1	2	3	3	3	2	3	1.257	25.66
1	2	3	4	4	2	4	1.238	23.79
2	3	6	6	6	3	6	2.370	18.49
2	3	6	7	6	4	7	2.353	17.65
2	3	6	7	7	4	7	2.302	15.09
4	6	12	13	12	7	13	4.592	14.81
4	6	12	13	13	7	14	4.584	14.60
4	6	12	14	13	7	14	4.581	14.52
5	8	15	17	16	9	17	5.703	14.06
6	9	18	20	19	11	21	6.834	13.90
6	9	18	21	19	11	21	6.815	13.59
10	15	30	34	32	18	35	11.343	13.43

Table 1. $3 \times 3 \times 3$ chamfer mask coefficients for anisotropic grid.

5 Results

Table 1 presents optimal sets of weights of a $3 \times 3 \times 3$ chamfer mask for an anisotropic grid with $dx = 1, dy = 1.5, dz = 3.0$. The points belonging to this mask are: $aX(1,0,0), aY(0,1,0), aZ(0,0,1), bYZ(0,1,1), bXZ(1,0,1), bXY(1,1,0)$, and $c(1,1,1)$. The time needed to compute these sets is 958 ms.

[1] Java code is available from `http://www-sop.inria.fr/epidaure/personnel/Celine.Fouard/`.

Table 2 presents optimal sets of weights the associated maximum relative error for $7 \times 7 \times 7$ isotropic chamfer masks. The points belonging to this mask are: $a(1,0,0)$, $b(1,1,0)$, $c(1,1,1)$, $d(2,1,0)$, $e(2,1,1)$, $f(2,2,1)$, $g(3,1,0)$, $h(3,1,1)$, $i(3,2,0)$, $j(3,2,1)$, $k(3,2,2)$, $l(3,3,1)$, $m(3,3,2)$. The computational times needed to examine all the m-tuples with ω_1 less or equal to 5, 7, 10, and 14 are respectively of 2 min, 25 min, 6 h 37 mn, and 102 h.

a	b	c	d	e	f	g	h	i	j	k	l	m	ε_{opt}	$\tau_{opt}(\%)$
1	1	1	2	2	2	3	3	3	3	3	3	3	1.211	21.13
1	2	2	3	3	4	4	4	5	5	5	6	6	1.207	20.71
2	2	3	4	4	5	6	6	6	6	7	7	8	2.293	14.64
2	3	3	5	5	6	7	7	8	8	8	9	9	2.252	12.60
2	3	4	5	6	7	7	8	8	9	10	10	11	2.225	11.24
3	4	5	6	7	9	9	9	10	11	12	13	14	3.158	5.28
4	6	7	9	10	13	13	14	15	16	17	19	20	4.179	4.49
5	7	9	11	12	15	16	16	18	19	21	22	24	5.186	3.72
5	7	9	11	12	15	16	17	18	19	21	22	24	5.149	2.97
7	10	12	16	17	21	22	23	26	27	29	31	33	7.176	2.51
8	11	14	18	19	24	25	26	29	30	33	34	38	8.184	2.30
10	14	17	22	24	30	32	33	36	37	41	43	47	10.224	2.24
12	17	21	27	29	36	38	40	44	45	49	52	56	12.245	2.04
14	20	24	31	34	43	44	46	51	53	58	62	67	14.248	1.77

Table 2. $7 \times 7 \times 7$ chamfer mask coefficients.

6 Conclusion

We have proposed an automated approach to compute optimal chamfer norm coefficients for mask of any size and for lattice of any anisotropy. It is based on the Farey triangulation that permits us to recursively build large masks while ensuring a regular triangulation of the chamfer mask generators. It allows us to automatically compute the error of any mask, thanks to analytical expressions of errors we can derive on regular cones. In addition, the coefficients we calculate verify norm constraints, thus yields scale invariant chamfer maps.

References

1. C.J. Pudney. Distance-ordered homotopic thinning: A skeletonization algorithm for 3d digital images. *CVIU*, 72(3):404–413, 1998.
2. G.T. Herman, J. Zheng, and C.A. Bucholtz. Shape-based interpolation. *IEEE Computer Graphics & Applications*, pages 69–79, 1992.
3. F.Y Shih and O.R. Mitchell. A mathematical morphology approach to euclidean distance transformation. *IEEE Trans. on Image Processing*, 1(2):197–204, 1992.
4. C.T. Huang and O.R. Mitchel. A euclidean distance transform using grayscale morphology decomposition. *IEEE Trans. on PAMI*, 16(4):443–448, 1994.
5. T. Saito and J.I. Toriwaki. New algorithms for euclidean distance transformation of an n-dimensional digitized picture with applications. *Pattern Recognition*, 27(11):1551–1565, 1994.

6. T. Hirata. A unified linear-time algorithm for computing distance maps. *Information Processing Letters*, 58:129–133, 1996.
7. P.E. Danielsson. Euclidean distance mapping. *CGIP*, 14:227–248, 1980.
8. I. Ragnemalm. The euclidean distance transform in arbitrary dimensions. *PRL*, 14(11):883–888, 1993.
9. G. Borgefors. Distance transformations in digital images. *CVGIP*, 34(3):344–371, 1986.
10. G. Borgefors. Distance transformations in arbitrary dimensions. *CVGIP*, 27:321–345, 1984.
11. B.J.H Verwer. Local distances for distance transformations in two and three dimensions. *PRL*, 12:671–682, 1991.
12. G. Borgefors. On digital distance transforms in three dimensions. *CVIU*, 64(3):368–376, 1996.
13. D. Coquin and Ph. Bolon. Discrete distance operator on rectangular grids. *PRL*, 16:911–923, 1995.
14. J.F. Mangin, I. Bloch, J. López-Krahe, and V. Frouin. Chamfer distances in anisotropic 3D images. In *VII European Signal Processing Conference*, Edimburgh, UK, 1994.
15. I.M. Sintorn and G. Borgefors. Weighted distance transfoms for images using elongated voxel grids. In *Proceedings of DGCI*, pages 244–254, 2002. LNCS 2301.
16. E. Remy. Optimizing 3d chamfer masks with norm constraints. In *IWCIA*, pages 39–56, July 2000.
17. A. Rosenfeld and J.L. Pfaltz. Sequential operations in digital picture processing. *JACM*, 13(4):471–494, 1966.
18. G.H. Hardy and E.M. Wright. *An Introduction to the Theory of Numbers*. Oxford University Press, 1978.
19. E. Thiel. *Les distances de chanfrein en analyse d'images : fondements et applications*. PhD thesis, Université Joseph Fourier, 1994.
20. E. Remy. *Normes de chanfrein et axe médian dans le volume discret*. PhD thesis, Université de la Méditerranée, Marseille, France, 2001.

A Recursive Farey triangulation construction

A.1 Farey Set Points

A Farey set $\widehat{\mathcal{F}}_n$ of order n is a set of all the irreducible points $\left(\frac{y}{x}, \frac{z}{x}\right)$ in $\mathbb{Q} \cap [0,1]$ whose denominator does not exceed n. It is built only with visible points (this means the greatest common divisor of (x, y, z) is 1).

A Farey set of order n correspond to the vectors of the generator of a 3-D chamfer mask of size $(2n+1)^3$. For example, the ordered (lexicographical order) Farey set of order 1 $\widehat{\mathcal{F}}_1 = \{(\frac{0}{1}, \frac{0}{1}), (\frac{1}{1}, \frac{0}{1}), (\frac{1}{1}, \frac{1}{1})\}$ correspond to the set of vectors $\{(1,0,0), (1,1,0), (1,1,1)\}$ which is the generator of an isotropic chamfer mask of size 3^3. Other vectors that are involved in an anisotropic chamfer mask are deduced from the previous ones by symmetries.

The Farey set of order $n+1$, $\widehat{\mathcal{F}}_{n+1}$, can be built from $\widehat{\mathcal{F}}n$ by

$$\widehat{\mathcal{F}}_{n+1} = \widehat{\mathcal{F}}_n \cup \left\{ \left(\frac{y}{x}, \frac{z}{x}\right) \widehat{+} \left(\frac{y'}{x'}, \frac{z'}{x'}\right) \text{ with } x + x' \leq n \text{ and } \left(\frac{y}{x}, \frac{z}{x}\right), \left(\frac{y'}{x'}, \frac{z'}{x'}\right) \in \widehat{\mathcal{F}}_n \right\}$$

the *addition* being defined by $\left(\frac{y}{x}, \frac{z}{x}\right) \widehat{+} \left(\frac{y'}{x'}, \frac{z'}{x'}\right) = \left(\frac{y+y'}{x+x'}, \frac{z+z'}{x+x'}\right)$ [18].

A.2 Recursive construction of Farey Set triangulations

The triangulation $\mathcal{T}_1$ associated to $\widehat{\mathcal{F}}_1$ is composed of a single cone $\langle\langle(1,0,0),(1,1,0),(1,1,1)\rangle\rangle$, or equivalently a Farey triangle $\langle\langle(\frac{0}{1},\frac{0}{1}),(\frac{1}{1},\frac{0}{1}),(\frac{1}{1},\frac{1}{1})\rangle\rangle$, that is regular.

To build $\mathcal{T}_{n+1}$ from $\mathcal{T}_n$, we first put all the Farey triangle in a list $\mathcal{L}$. We now examine successively the triangle in $\mathcal{L}$, and will try to build new triangles by splitting the existing one into two triangles.

Let us consider the triangle $\langle\langle A,B,C\rangle\rangle$ of $\mathcal{L}$. We try to add a new vertex along its largest edge[2], say AB. Such a vertex belongs to $\mathcal{F}_{n+1}$ if and only if $x_a + x_b \leq n+1$. If the latter is not true, the triangle is put again in the list but will no more be considered. If $x_a + x_b \leq n+1$ is true, let us denote $C' = A\widehat{+}B$ the new Farey point: the two triangles $\langle\langle A,C,C'\rangle\rangle$ and $\langle\langle B,C,C'\rangle\rangle$ are put into the list $\mathcal{L}$. It can also recursively be shown that those two triangles are regular.

The construction of $\mathcal{T}_{n+1}$ stops when no more triangles, whose vertices are Farey points of order $n+1$, can be inserted into $\mathcal{L}$.

Figure 3 shows the different steps of the construction of $\mathcal{T}_2$ from $\mathcal{T}_1$. $\mathcal{T}_3$ and

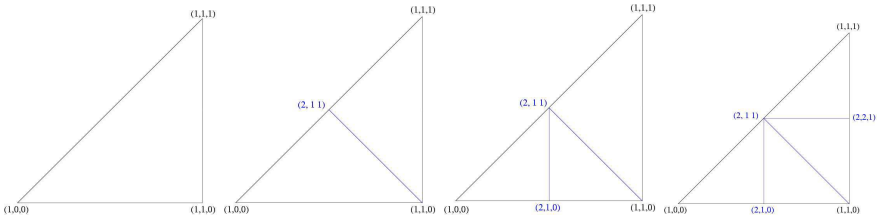

Fig. 3. Construction of $\mathcal{T}_2$ from $\mathcal{T}_1$.

$\mathcal{T}_4$ are displayed in Figure 4.

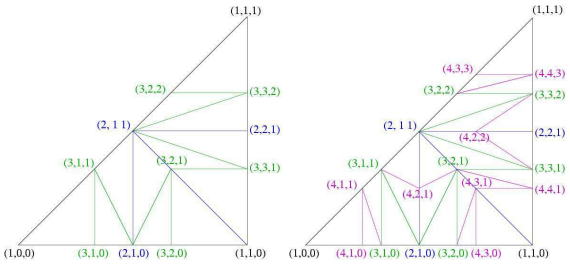

Fig. 4. $\mathcal{T}_3$ and $\mathcal{T}_4$.

[2] We consider that large discrepancies between the chamfer distance and the Euclidean one are more likely to occur along the largest edges.